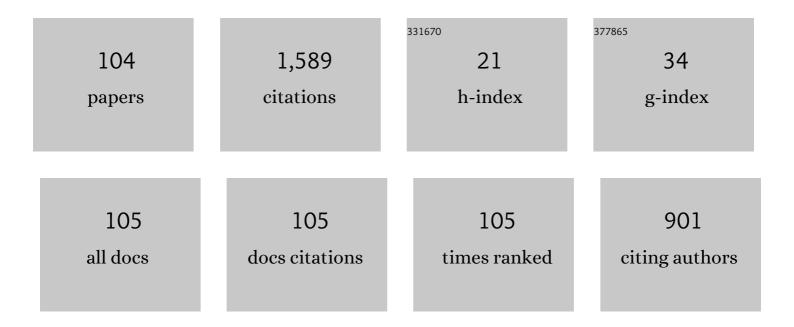
Xiao-Ming Duan

List of Publications by Year in descending order

Source: https://exaly.com/author-pdf/4152155/publications.pdf Version: 2024-02-01



#	Article	lF	CITATIONS
1	103ÂW in-band dual-end-pumped Ho:YAG laser. Optics Letters, 2012, 37, 3558.	3.3	87
2	Atomically Thin Hexagonal Boron Nitride and Its Heterostructures. Advanced Materials, 2021, 33, e2000769.	21.0	71
3	A 41-W ZnGeP_2 optical parametric oscillator pumped by a Q-switched Ho:YAG laser. Optics Letters, 2014, 39, 6589.	3.3	67
4	Active/passive Q-switching operation of 2  î¼m Tm,Ho:YAP laser with an acousto-optical Q-switch/MoS ₂ saturable absorber mirror. Photonics Research, 2018, 6, 614.	7.0	61
5	High power, tunable mid-infrared BaGa_4Se_7 optical parametric oscillator pumped by a 21 μm Ho:YAG laser. Optics Express, 2016, 24, 6083.	3.4	57
6	Singleâ€Phase Mixed Transition Metal Carbonate Encapsulated by Graphene: Facile Synthesis and Improved Lithium Storage Properties. Advanced Functional Materials, 2018, 28, 1705817.	14.9	56
7	Interplay between storage temperature, medium and leaching kinetics of hazardous wastes in Metakaolin-based geopolymer. Journal of Hazardous Materials, 2020, 384, 121377.	12.4	51
8	High repetition rate 102  W middle infrared ZnGeP ₂ master oscillator power amplifier system with thermal lens compensation. Optics Letters, 2019, 44, 715.	3.3	50
9	Continuous-wave and Q-switched operation of a resonantly pumped Ho:YAlO_3 laser. Optics Express, 2008, 16, 14668.	3.4	44
10	Safe trapping of cesium into doping-enhanced pollucite structure by geopolymer precursor technique. Journal of Hazardous Materials, 2019, 367, 577-588.	12.4	43
11	161  W middle infrared ZnGeP ₂ MOPA system pumped by 300  W-class Ho:YAG M Optics Letters, 2021, 46, 82.	MQPA syst	iem 41
12	High efficient actively Q-switched Ho:LuAG laser. Optics Express, 2009, 17, 21691.	3.4	40
13	High-power Cr^2+:ZnS saturable absorber passively Q-switched Ho:YAG ceramic laser and its application to pumping of a mid-IR OPO. Optics Letters, 2015, 40, 348.	3.3	38
14	Room temperature efficient actively Q-switched Ho:YAP laser. Optics Express, 2009, 17, 4427.	3.4	37
15	231  W dual-end-pumped Ho:YAG MOPA system and its application to a mid-infrared ZGP OPO. Optics Letters, 2018, 43, 5989.	3.3	35
16	High-efficiency, tunable 8-9 μm BaGa ₄ Se ₇ optical parametric oscillator pumped at 21 μm. Optical Materials Express, 2018, 8, 3332.	3.0	33
17	Microstructural evolution and mechanical properties of in situ nano Ta4HfC5 reinforced SiBCN composite ceramics. Journal of Advanced Ceramics, 2020, 9, 739-748.	17.4	28
18	<i>In Situ</i> Processing of Graphene/Leucite Nanocomposite Through Graphene Oxide/Geopolymer. Journal of the American Ceramic Society, 2016, 99, 1164-1173.	3.8	27

#	Article	IF	CITATIONS
19	Highly Dense Amorphous Si ₂ BC ₃ N Monoliths with Excellent Mechanical Properties Prepared by High Pressure Sintering. Journal of the American Ceramic Society, 2015, 98, 3782-3787.	3.8	24
20	Immobilization behavior of Sr in geopolymer and its ceramic product. Journal of the American Ceramic Society, 2020, 103, 1372-1384.	3.8	24
21	Solvents adjusted pure phase CoCO3 as anodes for high cycle stability. Journal of Advanced Ceramics, 2021, 10, 509-519.	17.4	22
22	Continuous-wave laser action around 2-μm in Ho^3+:Lu_2SiO_5. Optics Express, 2009, 17, 12582.	3.4	20
23	Influence of sintering pressure on the crystallization and mechanical properties of BN-MAS composite ceramics. Journal of Materials Science, 2016, 51, 2292-2298.	3.7	20
24	Active Q-switching operation of slab Ho:SYSO laser wing-pumped by fiber coupled laser diodes. Optics Express, 2019, 27, 11455.	3.4	20
25	Effect of the BN content on the thermal shock resistance and properties of BN/SiO ₂ composites fabricated from mechanically alloyed SiBON powders. RSC Advances, 2017, 7, 48994-49003.	3.6	18
26	High-beam-quality 2.1  µm pumped mid-infrared type-II phase-matching BaGa ₄ Se _{7<!--<br-->optical parametric oscillator with a ZnGeP₂ amplifier. Optics Letters, 2020, 45, 3805.}	sup>	17
27	570â€MHz harmonic mode-locking in an all polarization-maintaining Ho-doped fiber laser. Optics Express, 2020, 28, 33028.	3.4	17
28	Crystallization Behavior of Amorphous Si ₂ BC ₃ N Ceramic Monolith Subjected to High Pressure. Journal of the American Ceramic Society, 2015, 98, 3788-3796.	3.8	16
29	CdSe optical parametric oscillator operating at 12.07 µm with 170 mW output. Optics and Laser Technology, 2017, 92, 1-4.	4.6	16
30	3.5  W long-wave infrared ZnGeP ₂ optical parametric oscillator at 9.8  µm. Optic 2020, 45, 2347.	s Letters,	16
31	Research on performance improvement technology of a BaGa ₄ Se ₇ mid-infrared optical parametric oscillator. Optics Letters, 2020, 45, 6418.	3.3	16
32	114 W long-wave infrared source based on ZnGeP ₂ optical parametric amplifier. Optics Express, 2018, 26, 30195.	3.4	15
33	Microstructures, mechanical properties and oxidation resistance of SiBCN ceramics with the addition of MgO, ZrO ₂ and SiO ₂ (MZS) as sintering additives. RSC Advances, 2015, 5, 52194-52205.	3.6	14
34	A passively Q-switched Ho:YVO4 Laser at 2.05 μm with Graphene Saturable Absorber. Applied Sciences (Switzerland), 2016, 6, 128.	2.5	14
35	First-principles study of the anisotropic thermal expansion and thermal transport properties in h-BN. Science China Materials, 2021, 64, 953-963.	6.3	14
36	Stable passively Q-switched Ho:LuAG laser with graphene as a saturable absorber. Optical Engineering, 2014, 53, 126112.	1.0	13

#	Article	IF	CITATIONS
37	A passively Q-switching of diode-pumped 2.08-µm Ho:CaF2 laser. Infrared Physics and Technology, 2019, 103, 103071.	2.9	13
38	Efficient intracavity-pumped Ho:SSO laser with cascaded in-band pumping scheme. Infrared Physics and Technology, 2018, 94, 7-10.	2.9	12
39	Efficient Ho:YAP laser dual end-pumped by a laser diode at 1.91µm in a wing-pumping scheme. Applied Physics B: Lasers and Optics, 2018, 124, 1.	2.2	12
40	A high-beam-quality passively Q-switched 2Âμ m solid-state laser with a WSe2 saturable absorber. Optics and Laser Technology, 2020, 125, 105960.	4.6	12
41	1  W, 10.1  µm, CdSe optical parametric oscillator with continuous-wave seed injection. Optic 2020, 45, 2119.	s Letters,	11
42	A ring ZnGeP2 optical parametric oscillator pumped by a Ho:LuAG laser. Applied Physics B: Lasers and Optics, 2014, 117, 127-130.	2.2	10
43	Passive Q-switched operation of an <i>a</i> -cut Tm,Ho:YAP laser with a few-layer WS ₂ saturable absorber. Laser Physics Letters, 2018, 15, 085806.	1.4	10
44	From bulk to porous structures: Tailoring monoclinic SrAl ₂ Si ₂ O ₈ ceramic by geopolymer precursor technique. Journal of the American Ceramic Society, 2020, 103, 4957-4968.	3.8	10
45	Effects of Li Substitution on the Microstructure and Thermal Expansion Behavior of Pollucite Derived from Geopolymer. Journal of the American Ceramic Society, 2016, 99, 3784-3791.	3.8	9
46	Corrosion behavior and microstructural evolution of <scp>BN</scp> –ZrO ₂ –SiC composites in molten steel. International Journal of Applied Ceramic Technology, 2017, 14, 665-674.	2.1	9
47	High-power actively Q-switched Ho-doped gadolinium tantalate laser. Optics Express, 2021, 29, 12471.	3.4	9
48	High-beam-quality operation of a 2  μm passively Q-switched solid-state laser based on a boron nitride saturable absorber. Applied Optics, 2019, 58, 2546.	1.8	9
49	Resonantly pumped high efficiency Ho:GdTaO ₄ laser. Optics Express, 2019, 27, 18273.	3.4	9
50	High efficiency single-longitudinal-mode resonantly-pumped Ho:GdTaO ₄ laser at 2068nm. Optics Express, 2019, 27, 34204.	3.4	9
51	11 Âμm, high beam quality idler-resonant CdSe optical parametric oscillator with continuous-wave injection-seeded at 2.58 Âμm. Optics Express, 2020, 28, 17056.	3.4	9
52	A 52-mJ Ho:YAG Master Oscillator and Power Amplifier with Kilohertz Pulse Repetition Frequency. Chinese Physics Letters, 2014, 31, 094201.	3.3	8
53	Synthesis of Novel Cobalt-Containing Polysilazane Nanofibers with Fluorescence by Electrospinning. Polymers, 2016, 8, 350.	4.5	8
54	Effects of Na ⁺ substitution Cs ⁺ on the microstructure and thermal expansion behavior of ceramic derived from geopolymer. Journal of the American Ceramic Society, 2017, 100, 4412-4424.	3.8	8

#	Article	IF	CITATIONS
55	Carbon content-dependent microstructures, surface characteristics and thermal stability of mechanical alloying derived SiBCN powders. Ceramics International, 2018, 44, 3614-3624.	4.8	8
56	Study on long-wave infrared ZnGeP2 subsequent optical parametric amplifiers with different types of phase matching of ZnGeP2 crystals. Applied Physics B: Lasers and Optics, 2019, 125, 1.	2.2	8
57	Wavelength-locked continuous-wave and Q-switched Ho:CaF ₂ laser at 21005 nm. Optics Express, 2018, 26, 26916.	3.4	8
58	Growth, spectra and continuous-wave 2.1 μm laser operation of a Ho ³⁺ -doped bismuth silicate crystal. CrystEngComm, 2022, 24, 1590-1597.	2.6	8
59	High power slab Tm:YAP laser dual-end-pumped by fiber coupled laser diodes. Optical and Quantum Electronics, 2015, 47, 1055-1061.	3.3	7
60	Microstructure and erosion resistance of in-situ SiAlON reinforced BN-SiO2 composite ceramics. Journal Wuhan University of Technology, Materials Science Edition, 2016, 31, 315-320.	1.0	7
61	Efficient middle-infrared ZGP-OPO pumped by a Q-switched Ho:LuAG laser with the orthogonally polarized pump recycling scheme. Applied Optics, 2018, 57, 8102.	1.8	7
62	Passively <i>Q</i> -switched operation of a Tm:YAlO ₃ laser with a BN saturable absorber mirror. Laser Physics Letters, 2019, 16, 025801.	1.4	7
63	Thermal lens effect and laser characteristics of Ho:YAG ceramic laser with a concave-convex cavity. Optik, 2020, 221, 165307.	2.9	7
64	Effects of Zr and chopped C fiber on microstructure and mechanical properties of SiBCN ceramics. Science China Technological Sciences, 2020, 63, 1520-1530.	4.0	7
65	Efficient Ho:(Sc ₀₅ Y ₀₅) ₂ SiO ₅ laser at 21 µm in-band pumped by Tm fiber laser. Optics Express, 2019, 27, 4522.	3.4	7
66	Continuously tunable high-power single-longitudinal-mode Ho:YLF laser around the P12 CO ₂ absorption line. Optics Letters, 2020, 45, 6691.	3.3	7
67	Hardness and toughness improvement of SiCâ€based ceramics with the addition of (Hf _{0.2} Mo _{0.2} Ta _{0.2} Nb _{0.2} Ti _{0.2} B ₂ . Journal of the American Ceramic Society, 2022, 105, 1629-1634.	3.8	7
68	High power Ho:YAG laser pumped by two orthogonally polarized Tm:YLF lasers. Optical and Quantum Electronics, 2015, 47, 211-216.	3.3	6
69	Geopolymer-Encapsulated Cesium Lead Bromide Perovskite Nanocrystals for Potential Display Applications. ACS Applied Nano Materials, 2020, 3, 11695-11700.	5.0	6
70	Passively Q-switched Tm:YAP laser with a lead zirconate titanate saturable absorber. Applied Optics, 2021, 60, 8097.	1.8	6
71	Thermal-birefringence-induced depolarization in a 450 W Ho:YAG MOPA system. Optics Express, 2022, 30, 21501.	3.4	6
72	2130.7 nm, Single-Frequency Q-Switched Operation of Tm,Ho:YAlO\$_{3}\$ Laser Injection-Seeded by a Microchip Tm,Ho:YAlO\$_{3}\$ Laser. Applied Physics Express, 2012, 5, 082702.	2.4	5

#	Article	IF	CITATIONS
73	High-Power in-Band Pumped a-Cut Ho:Yap Laser. Journal of Russian Laser Research, 2014, 35, 239-243.	0.6	5
74	A 2 μm Single-Longitudinal-Mode Ho:GdVO4 CW Laser. Journal of Russian Laser Research, 2021, 42, 355.	0.6	5
75	202 W dual-end-pumped Tm:YLF laser with a VBG as an output coupler. High Power Laser Science and Engineering, 2021, 9, .	4.6	5
76	Tm ³⁺ : Bi ₄ Si ₃ O ₁₂ crystal as a promising laser material near 2 l¼m: growth, spectroscopic properties and laser performance. Optics Express, 2021, 29, 29138.	3.4	5
77	Watt-level long-wave infrared CdSe pulsed-nanosecond optical parametric oscillator. Optics and Laser Technology, 2022, 145, 107491.	4.6	5
78	Measurement of optical homogeneity of ZnGeP ₂ crystal using a 2.02 µm single-longitudinal-mode Tm:LuAG ring laser. Applied Optics, 2020, 59, 5864.	1.8	5
79	1104  mJ, 1  kHz repetition rate, Ho:YAG master oscillator power amplifier. Applied Optics, 201	9,1 5 8, 87	' 9. 5
80	Single-longitudinal-mode Ho:YVO4 MOPA system with a passively Q-switched unidirectional ring oscillator. Optics Express, 2019, 27, 34618.	3.4	5
81	Preparation and mechanical performance of SiC w /geopolymer composites through direct ink writing. Journal of the American Ceramic Society, 0, , .	3.8	5
82	Influence of sintering temperature on the crystallization and mechanical properties of BNâ€MAS composites. Journal of the American Ceramic Society, 2022, 105, 3590-3600.	3.8	5
83	An efficient, compact Ho:YLF MOPA system pumped by a linearly polarized Tm:YAP laser. Optics and Laser Technology, 2022, 150, 107977.	4.6	5
84	113  W Ho:YLF oscillator with good beam quality efficiently pumped by a Tm:YAP laser. Applied Optics, 2022, 61, 5755.	1.8	5
85	A 2.22-W Passively Q-Switched Tm ³⁺ -Doped Laser With a TiC ₂ Saturable Absorber. IEEE Photonics Journal, 2019, 11, 1-7.	2.0	4
86	Comparison of mid-infrared ZnGeP ₂ rectangle ring optical parametric oscillators of three types of resonant regimes. Applied Optics, 2019, 58, 4163.	1.8	4
87	1ÂkHz, 1.5ÂMW peak power pulse generation from an acousto-optically Q-switched Ho:GdVO4 oscillator. Optics and Laser Technology, 2022, 152, 108114.	4.6	4
88	A Mid-Irfrared Rectangle Ring OPO Pumped by an Actively/Passively Q-Switched 2.09 μm Polycrystalline Laser. Journal of Russian Laser Research, 2022, 43, 224-228.	0.6	4
89	Resonantly pumped high power acousto-optical Q-switched Ho:YAG ceramic laser. Optik, 2016, 127, 1595-1598.	2.9	3
90	Carbon ontentâ€dependent phase composition, microstructural evolution, and mechanical properties of Si <scp>BCN</scp> monoliths. Journal of the American Ceramic Society, 2018, 101, 2137-2154.	3.8	3

#	Article	IF	CITATIONS
91	High power passively Q-switched Tmc+:(LuxGd1-x)3Ga5O12 laser based on boron nitride. Optics and Laser Technology, 2020, 123, 105795.	4.6	3
92	Microstructure and Hydrophobic Properties of Nano-Cu-Coated Wood-Based Composites by Ultrasonic Pretreatment. Applied Sciences (Switzerland), 2020, 10, 5448.	2.5	3
93	Broadband second-harmonic and sum-frequency generation with a long-wave infrared laser in AgGaGe ₅ Se ₁₂ . Applied Optics, 2020, 59, 5247.	1.8	3
94	High power narrow-linewidth Tm:YLF slab laser with volume Bragg grating and Fabry-Perot etalon. Optical Review, 2014, 21, 775-777.	2.0	2
95	Investigation of a gain-switched Cr2+: ZnSe laser pumped by an acousto-optic Q-switched Ho : YAG laser. Quantum Electronics, 2016, 46, 772-776.	1.0	2
96	High-Power Continuous-Wave and Acousto-Optical Q-Switched Ho:(Sc0.5Y0.5)2SiO5 Laser Pumped by Laser Diode. Chinese Physics Letters, 2019, 36, 064201.	3.3	2
97	Tunable twisted-mode Ho:YAG laser at continuous-wave and pulsed operation. Optics Express, 2020, 28, 31775.	3.4	2
98	High-repetition-rate laser ultrasonic generation in carbon-fiber-reinforced plastics excited by a 32–34  μm ZGP master oscillator power amplifier system. Applied Optics, 2019, 58, 7655.	1.8	2
99	11.6 W middle infrared ZnGeP2 optical parametric amplifier system with a 1 kHz repetition rate. Laser Physics, 2020, 30, 095001.	1.2	2
100	High-Power Dual-End-Pumped Monolithic Tm:YAP Microlaser. Journal of Russian Laser Research, 2019, 40, 382-385.	0.6	1
101	Tunable single-longitudinal-mode resonantly-pumped Ho:YAP unidirectional ring laser. Optical and Quantum Electronics, 2021, 53, 1.	3.3	1
102	Resonantly pumped high efficiency Ho:GdTaO4 laser: erratum. Optics Express, 2019, 27, 31362.	3.4	1
103	Acousto-optic mode-locked Tm:LuAG laser with nearly diffraction-limited beam. Optical and Quantum Electronics, 2019, 51, 1.	3.3	0
104	Editorial for the Special Issue on "Advances in Middle Infrared Laser Crystals and Its Applications― Crystals, 2022, 12, 643.	2.2	0